**Supplementary Figures**

**Figure S1. Hierarchical oxidative stress paradigm**

We have previously demonstrated that metal oxide nanoparticles are capable of generating ROS and inducing cellular oxidant injury according to the tenets of the hierarchical oxidative stress model [1, 2]. According to this model, lower levels of oxidative stress (Tier 1) are capable of activating phase 2 and antioxidant enzyme expression through the activation of an antioxidant response element in the promoters of these genes. This Nrf2-mediated response is protective and attempts to restore redox equilibrium through increased synthesis of glutathione as well as increased expression of oxygen scavenging enzymes. If there is a failure to restore redox equilibrium, higher levels of oxidative stress (Tier 2), capable of activating MAPK and NF-κB cascades induce pro-inflammatory responses, *e.g*., cytokine and chemokine production. These inflammatory effects contribute to disease processes such as asthma and atherosclerosis. Upon further escalation of oxidative stress (Tier 3), the triggering of intracellular $Ca^{2+}$ release, interference in mitochondrial inner membrane electron transduction and large scale opening of the mitochondrial permeability transition pore can lead to cytotoxicity, either through the release of apoptotic factors or failure to produce ATP. This could result in cellular apoptosis or apoptosis-necrosis. Our assay captures the events in the Tier 3 of the oxidative stress response.

**Figure S2. Assessment of ROS production by metal oxide NPs**

Cells grown in 384 multi-well plates were treated with NPs (6.125-50μg/mL) and loaded with H2-DCF-DA (15μmol) or MitoSox Red (5μM) for 20 min to quantify $H_2O_2$ and

mitochondrial superoxide generation. The cells were washed and analyzed using an epifluorescence microscope as described in materials and methods. The percentage of cells that exceed a set fluorescence threshold were scored as positive and plotted as percentage positive cells. In the Hoechst/DAPI channel the approximate minimum width was 3 µm (about 3 pixels) and the approximate maximum width was 10 µm (about 7 pixels). The intensity above background level was 100 gray levels. For the TRITC channels (red) the approximate minimum width was 5 µm (about 6 pixels) and the approximate maximum width is 30 µm (about 22 pixels). The intensity above background is 500 gray levels. Similar to our previously published data, ZnO nanoparticles induced $H_2O_2$ and mitochondrial superoxide in a concentration dependent fashion in BEAS-2B cells and RAW264.7 cells [3]. The data comparing non-treated with cells treated with 50µg/mL of the particles are shown.

*$p<0.05$

**Figure S3. Mechanism of ZnO NP mediated cytotoxicity**

ZnO nanoparticle dissolution leads to cellular uptake of $Zn^{++}$ as well as intracellular dissolution of the particle remnants in endosomal compartments, from where ion release leads to lysosomal damage, $[Ca^{2+}]_i$ flux, mitochondrial perturbation and cytotoxicity (left panel). The right side panel shows our hypothesis, namely that iron doping could lead to an improvement of toxicity due to a decreased rate of $Zn^{2+}$ release.

**Figure S4. Dissolution of $Zn^{2+}$ from iron doped ZnO NPs**

Dissolved zinc concentrations for undoped and Fe-doped nanoparticles after 10 days in PIPES buffered solution at pH 7.

**Figure S5. Proposed model for reducing $Zn^{2+}$ dissolution from ZnO NPs**

Proposed Model of *d*-orbital electronic configuration of Fe doped with ZnO NPs. $Fe^{3+}$ have much lower crystal field stabilization energy in both high spin and low spin cases compared with $Fe^{2+}$ suggesting a strong $Fe^{3+}$ covalency in the molecule which binds ZnO strongly (*d*2*sp*3 hybridisation) in the lattice so that the dissolution process is lowered compared to the individual ZnO.

**References**


1. Xia, T.; Kovochich, M.; Brant, J.; Hotze, M.; Sempf, J.; Oberley, T.; Sioutas, C.; Yeh, J. I.; Wiesner, M. R.; Nel, A. E., Comparison of the Abilities of Ambient and Manufactured Nanoparticles To Induce Cellular Toxicity According to an Oxidative Stress Paradigm. *Nano Letters* **2006,** 6, (8), 1794-1807.

2. Nel, A.; Xia, T.; Madler, L.; Li, N., Toxic Potential of Materials at the Nanolevel. *Science* **2006,** 311, (5761), 622-627.

3. Xia, T.; Kovochich, M.; Liong, M.; MaÌˆdler, L.; Gilbert, B.; Shi, H.; Yeh, J. I.; Zink, J. I.; Nel, A. E., Comparison of the Mechanism of Toxicity of Zinc Oxide and Cerium Oxide Nanoparticles Based on Dissolution and Oxidative Stress Properties. *ACS Nano* **2008,** 2, (10), 2121-2134.

**Figure S1.**

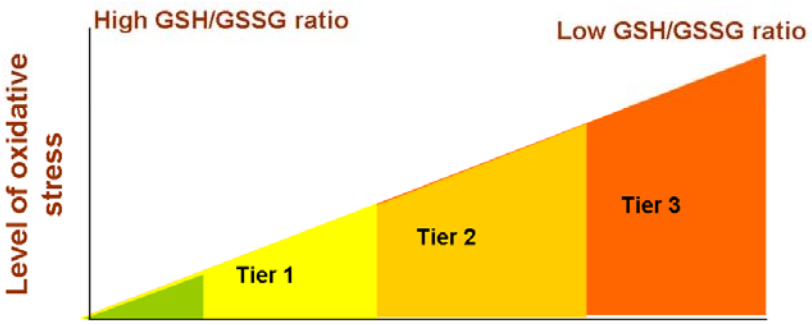


| Cell response pathway | Normal | Anti-oxidant Defense | Inflammation | Cytotoxicity |
|---|---|---|---|---|
| Signaling pathway: | | Nrf-2 | MAPK | Mitochondrial perturbation-PT pore |
| Genetic response: | | ARE | AP-1 | N/A |
| Outcome | | Phasell enzyme | Cytokines chemokines | Apoptosis |

**Figure S2.**

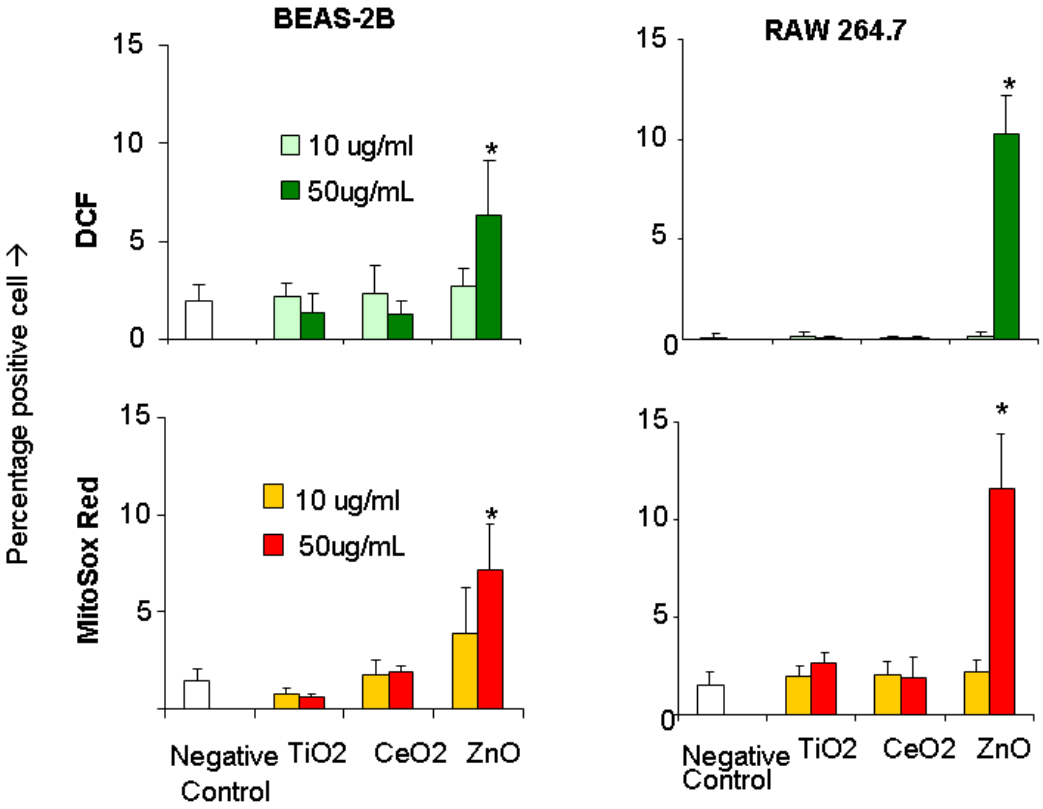
BEAS-2B
RAW 264.7
DCF
MitoSox Red
Percentage positive cell →
10 ug/ml
50ug/mL
15
10
5
0
*
Negative Control
TiO2
CeO2
ZnO

**Figure S3**

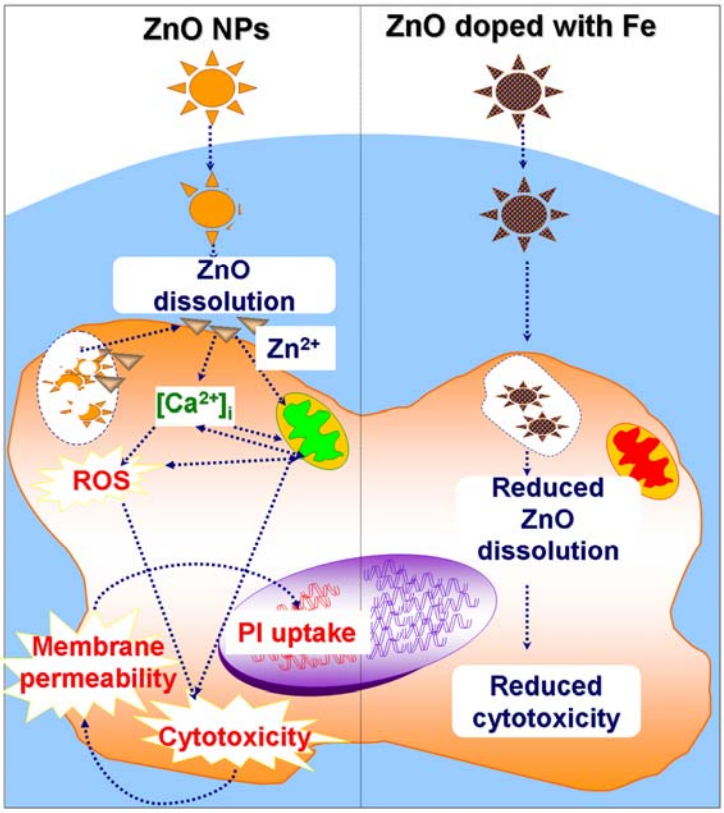
ZnO NPs
ZnO doped with Fe
ZnO dissolution
Zn2+
[Ca2+]i
ROS
Membrane permeability
PI uptake
Cytotoxicity
Reduced ZnO dissolution
Reduced cytotoxicity

**Figure S4.**

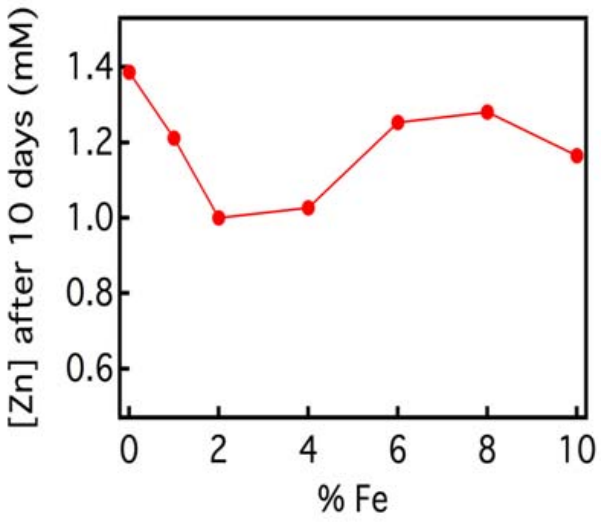

**Figure S5.**

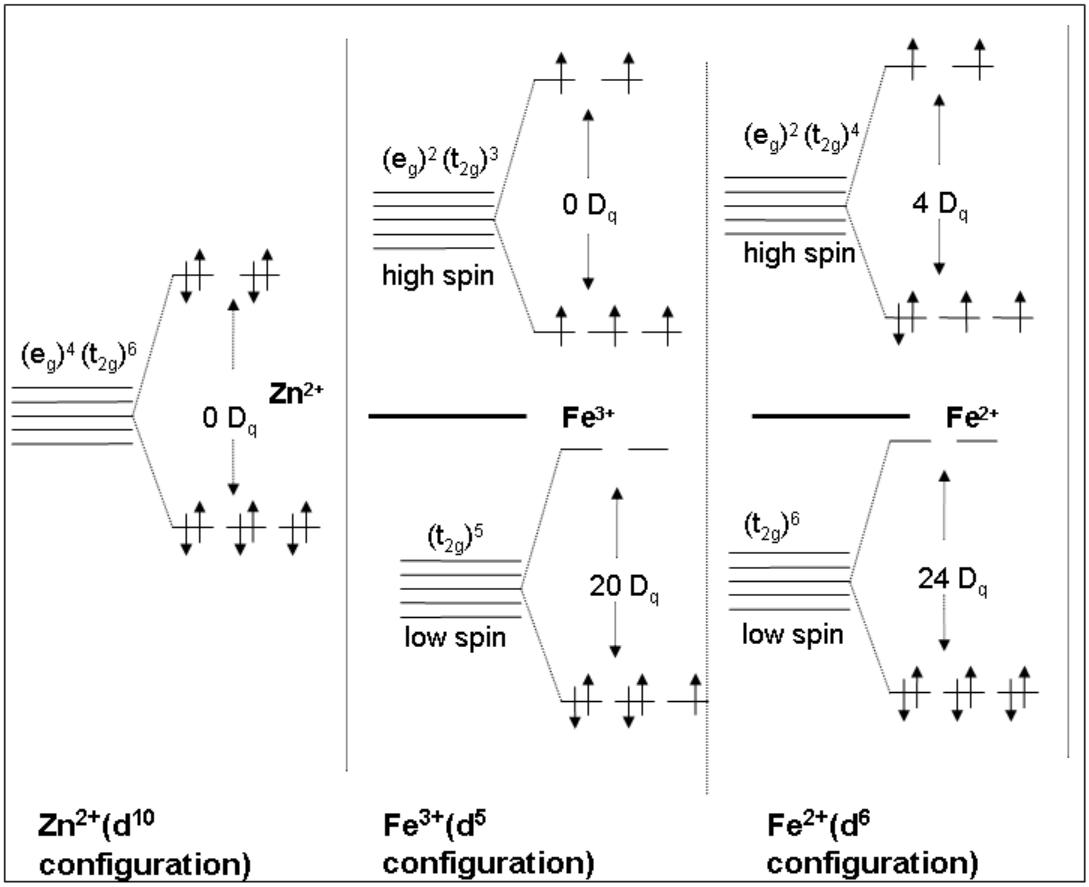
$(e_g)^4 (t_{2g})^6$
0 $D_q$
$Zn^{2+}$
$(e_g)^2 (t_{2g})^3$
0 $D_q$
high spin
$Fe^{3+}$
$(t_{2g})^5$
20 $D_q$
low spin
$(e_g)^2 (t_{2g})^4$
4 $D_q$
high spin
$Fe^{2+}$
$(t_{2g})^6$
24 $D_q$
low spin
$Zn^{2+}$($d^{10}$ configuration)
$Fe^{3+}$($d^5$ configuration)
$Fe^{2+}$($d^6$ configuration)